

# Petrogenesis and tectonomagmatic setting of gabbroic rocks in the Gisel area (northern Iran)

Farzaneh Farahi<sup>1</sup>, Saeed Taki<sup>2\*</sup>, Mojgan Salavati<sup>3</sup>

<sup>1,2,3</sup>Department of Geology, Faculty of Basic Sciences, Lahijan Branch, Islamic Azad University, Lahijan, Iran.

## Abstract

The Alborz-Azerbaijan magmatic zone in northern Iran is one of the important zones of magmatic activity in the Cenozoic. Lithologically, this complex consists of olivine gabbro, monzogabbro, dolerite, and gabbro with granular, intergranular, and porphyritic textures. The main phenocrysts of these rocks are clinopyroxene, plagioclase, and sometimes iddingsitized olivine. The rocks producing magma has potassic and shoshonitic nature. Enrichment in large-ion lithophile elements (LILEs), i.e., Ba, Rb, and Th, and depletion of high-field strength elements (HFSEs), i.e., Ti and Nb, in the spider diagrams are of the characteristics of subduction and active continental margin rocks. Also, these diagrams show enrichment in the light rare earth elements (LREEs) compared to heavy rare earth elements (HREEs). This feature also is representative of the rocks of subduction zones and active continental margins. The geochemical and petrogenetic studies indicate unique origin of the intrusive rocks in the study area and the role of fractional crystallization with simultaneous crustal assimilation (AFC) and magma contamination with crustal rocks in the evolution of the magma forming these rocks. This magma is obtained from the low-degree partial melting of an enriched mantle source beneath the continental lithosphere with garnet lherzolite composition at a depth of 100 to 110 km in a post-collision extensional basin.

**Keywords:** Basic intrusive rocks; Tectonic environment; Gisel, Central Alborz.

## INTRODUCTION

Alborz structural zone is the collisional zone of Gondwana to Eurasia. Therefore, it has long been extensively studied by several researchers (Stöcklin, 1974; Berberian & Berberian, 1981; Stampfli, 200; Guest et al., 2006a,b). The western Alborz on the northwestern side along the Alpine-Himalayan belt, reaches the Oligocene to Quaternary Kora Molasse Basin (Zanchi et al., 2006), and the Transcaucasus Molasse Basin in northeastern Turkey and the eastern part of the North Caucasus Molasse Basin (Ershov et al., 2003; Yazdi et al. 2019-a). Accordingly, several phases of orogeny, magmatic activity, and sedimentation from the Early Paleozoic to the present have been identified and studied in this zone. Here, the Cenozoic magmatism with basic to acidic (less frequently) composition has been highly active. The Alborz Cenozoic magmatic activity, which are mostly of Paleogene age, is equivalent to the Karaj Formation in stratigraphic divisions (Annells et al., 1975; Stöcklin, 1968; Yazdi et al. 2019-b).

According to some researchers, the rocks of the Karaj Formation are continental and subduction-related in the northern direction and along the Zagros (Zanchi, 2006; Asiabanha et al., 1989). Also, some have considered the age of equivalent units in western Qazvin equal to that of the Oligocene (Asiabanha, 2001). Following underwater explosive volcanic activities in Alborz, large masses of intermediate to basic lavas have erupted through surface fractures (Mobashergarmi, 2013). The origin of these volcanic lavas is a subduction zone with a small percentage of the asthenosphere (Shafaii Moghadam & Shahbazi Shiran, 2010).

Address for correspondence: Saeed Taki

Faculty of Basic Sciences, Lahijan Branch, Islamic Azad University, Lahijan, Iran.

Email: taki\_saeed2002@yahoo.com

This is an open access journal, and articles are distributed under the terms of the Creative Commons Attribution-NonCommercial-ShareAlike 4.0 License, which allows others to remix, tweak, and build upon the work non-commercially, as long as appropriate credit is given and the new creations are licensed under the identical terms.

For reprints contact: pnrjournal@gmail.com

How to cite this article: Farzaneh Farahi, Saeed Taki, Mojgan Salavati, Petrogenesis and tectonomagmatic setting of gabbroic rocks in the Gisel area (northern Iran), J PHARM NEGATIVE RESULTS 2022;13: 583-592.

### Access this article online

Quick Response Code:



Website:

www.pnrjournal.com

DOI:

10.47750/pnr.2022.13.04.077

The volcanic-plutonic assemblage of the Alborz region in northern Iran indicates the subduction of the Neo-Tethysian oceanic rock beneath the Central Iranian subcontinent and the subsequent continental collision between the Saudi and Iranian plates in the late Oligocene (Agard et al., 2011). However, recent studies on Tertiary magmatic activity in Alborz have shown the effect of subduction on magmatic activity. In this respect, various tectonic environments have been presented that can be attributed to continental arc magmatic activity (Valizadeh et al., 2008), the magmatic activity of subduction zones in the active continental margins (Rahimi et al., 2010), and the magmatic activity in the back-arc extensional zone (Asiabanha & Foden, 2012). According to Nemati & Asiabanha (2016), the plutonic masses of the Lat-Bolukan region (north of Qazvin) belong to the active continental margin and have formed in a volcanic arc. Also, Teimouri et al. (2018) believe that Jirandeh volcanic rocks (northwest of Qazvin) are dependent on the active volcanic continental arc.

### Methodology

In this section, we investigate and determine the amount of major, minor, and rare elements in the samples of the study area. To this end, different rock units with the least alteration were sampled over the field trips. Overall, 14 whole-rock samples were selected and were examined through inductively coupled plasma mass spectrometry (ICP-MS) in MS Analytical of Canada (Table 1).

### Geology of the study area

The study area is a part of the Alborz Mountains and belongs to the western part of the Central Alborz Zone. The geographical coordinates of this area are 50° 0' to 50° 49'E and 36° 47' to 36° 50'N. Tertiary rock units (Paleogene) are seen in the study area up to the present time. A large part of the area is covered by Eocene sedimentary-volcanic units, which are penetrated by intrusive masses in some locations. Eocene deposits include a sequence of volcanic and volcanoclastic rocks (Fig. 1). The mentioned volcanoclastic units (denoted in the geological map with Eat) consist of an alternation of acidic and intermediate tuffs, including lava layers with basic-intermediate composition and clastic layers (Baharfirooz et al., 2003; Yazdi et al. 2016; Gharib-Gorgani et al. 2017; Baratian et al. 2018; Jehangir Khan et al. 2021). The color of this unit is dark gray or red. This unit's tuffs are mostly rock-crystalline or crystalline-rock type with dacitic or andesitic composition with a porphyroclastic texture. The Eat unit contains lava windows or lenses marked on the map with the Evl symbol (Baharfirooz et al., 2003; Yazdi et al. 2022). These lavas have an intermediate to basic composition and often make an assemblage of basalt, basaltic andesite, trachyandesite, and andesite rocks (Fig. 1). Most intrusive rocks appear as small to medium stocks (approximately several meters to several hundred meters in diameter) or dikes (approximately 0.5 to 2-m wide and several tens of meters long). Exfoliation

is locally seen in these stocks. Most of the intrusive rocks in the study area are of the gabbroic composition, and the dikes are of quartz-diorite type. Along the contact of intrusive masses with intrusive rocks, there is often no specific phenomenon other than the presence of alteration zones. Because the studied intrusives have penetrated Eocene rock units, their age is younger than Eocene. The eruption of volcanic rocks in the area can be assumed to be in two phases. The first phase consists of rocks from magmas that have erupted in a shallow marine environment with little sediment. Most of the rocks of this stage are acidic and belonged to Eocene (equivalent to units 5 and 6 of Karaj Formation) (Asiabanha, 2001; Bina et al. 2020; Yazdi and sharifi teshnizi, 2021). The rocks of this phase are mostly acidic and andesitic green tuffs. The second phase consists mostly of intermediate to basic volcanic rocks and is often younger than Eocene. This magma has erupted in a dry environment and lacks associated sedimentary rocks. The second phase rocks include olivine basalt, basalt, andesitic basalt, trachyandesite, and rhyodacite. Eocene volcanic units are mostly composed of basaltic andesite, and younger lavas are mainly composed of olivine-basalt and basalt (Annells et al., 1975).

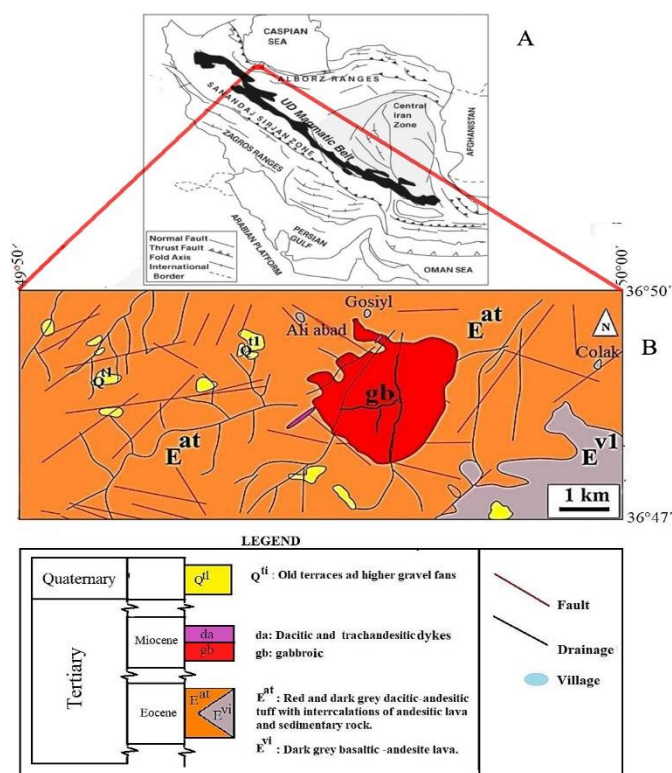


Figure 1. A: Location of the study area on the geological map of Iran (Modified from Gile et al. 2006). B: Simplified geology map of the study area (after Baharfirooz et al., 2002).

### Petrography and mineral geochemistry

Most rocks in the study area include gabbro, olivine gabbro, olivine monzogabbro, porphyritic gabbro, olivine dolerite. Phenocrystals often composed of plagioclase, pyroxene, alkaline feldspar, and olivine. The rock matrix often

comprises plagioclase microlites, opaque minerals, quartz, and cryptocrystalline minerals. These rocks represent a variety of porphyritic, trachytoid, intergranular, and sieve textures (Fig. 2). Accessory minerals include magnetite, titanomagnetite (opaque minerals) and apatite.

#### Plagioclases

Plagioclases have been mostly decomposed into sericite, chlorite, and clay minerals. Plagioclase, with an abundance of about 15 to 20%, is the second abundant mineral of these rocks. This mineral is often euhedral to subhedral in the form of fine to large blades with polysynthetic twins. These minerals sometimes show sericitization alteration. This alteration, which is mainly in the center of the crystal, shows the normal zonation of plagioclase and the higher Ca-rich core of the crystals compared to their margins. Point analysis of plagioclases and their cations were calculated based on octahedral oxygen formula. On the Or-Ab-An triangular diagram of Deer (1991), the plagioclases of the study area are plot in the andesine, labradorite, and bytownite fields (Fig. 3A). The chemical compositions of plagioclases crystals in gabbro vary from An<sub>14.22</sub>Ab<sub>80.92</sub>Or<sub>4.86</sub> to An<sub>84.14</sub>Ab<sub>15.31</sub>Or<sub>0.55</sub>. Zoning in plagioclase mineralization has formed for two reasons. First, plagioclase has been crystallized in a melt that undergoes continuous variations in temperature, water vapor pressure, and composition (magmatic mixing and change in magma chemical composition during magma crystallization) (Humphreys et al., 2006). Decreased pressure due to sudden magma ascension and increased oxygen escape are other factors changing the amount of anorthite plagioclase from the center to the edge (Blundy et al., 2006). The oxygen escape change due to successive injection of magma from the mantle into the magmatic chamber changes the chemical composition of the melt, so crystals in the magmatic chamber can lead to zoning. Second, increased growth rate at the crystal-melt interface in response to equilibrium conditions (Ginibre et al., 2002a) is the other explanation for this mineralization.

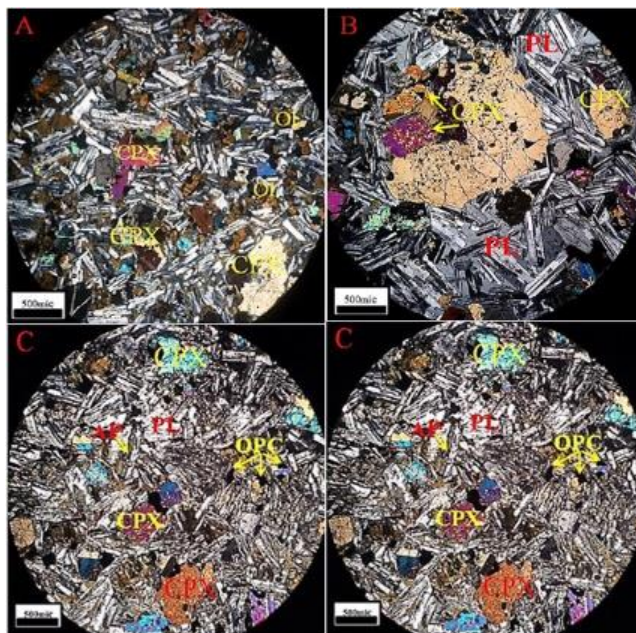


Fig. 2. A) Relatively fine-grained subhedral granular texture in olivine monzogabbro; B) Porphyritic texture in olivine monzogabbro; C) Subhedral granular texture in olivine gabbro; D) Trachytoid texture in olivine gabbro

#### Pyroxene

Clinopyroxene appeared as subhedral to euhedral with a frequency of about 42%, and is the most important and abundant mineral. Sometimes, they have been euralitized and is seen with cavities filled with chlorite. Morimoto et al. (1988) classification diagram was used to determine the type of pyroxenes. As shown in Fig. 3B, in the Q-J diagram, the studied pyroxenes are in the range of Fe-Mg-Ca type pyroxenes. Also, according to the Polderwaart-Hess diagram (Fig. 3C), the pyroxenes are in the composition range of augite, hypersthene, and Ferro-hypersthene. The chemical composition range of clinopyroxene phenocrysts in gabbro varies from En<sub>0.422</sub>Fs<sub>5.07</sub>Wo<sub>94.50</sub> to En<sub>61.14</sub>Fs<sub>34.98</sub>Wo<sub>3.86</sub> (Fig. 3C).

#### Olivine

Plotting of olivines microprobe data on various diagrams, including Wager & Deer (1939), show hialosiderite composition (Fig. 3D).

#### Alkali feldspars

The chemical formula of analyzed alkali feldspar sample is Or<sub>73</sub>Ab<sub>26</sub>An<sub>1</sub> (Fig. 3A).

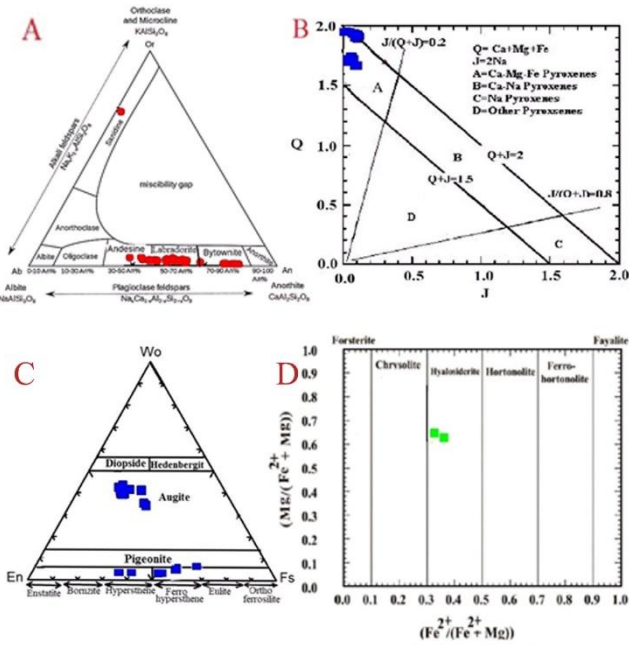


Fig. 3. A) The chemical composition classification diagram of feldspars and plotting of plagioclases and alkali feldspars of the study area on it. B) classification of pyroxenes in olivine gabbro based on Q-J indices; B) the position of the pyroxene data in the Polderwart-Hess diagram; C) The diagram to determine olivine composition

Geochemical studies

Chemical analysis of the gabbroic rocks of the Gisel area shows that the SiO<sub>2</sub> content of these rocks varies from 48.79 to 52.57 wt.% and according to the TAS diagram, the studied rocks rest in gabbro field and subalkaline shoshonitic series (Fig 3). According to Kelemen et al. (2004), basic samples with #mg<50, 60 to 50 and > 60 have been derived from the evolved parental magma, primary and high magnesium parental magma respectively. The magnesium numbers (#mg) of the collected samples are between 41 and 53 so they are mostly evolved. In general, the concentrations of MnO, CaO, P<sub>2</sub>O<sub>5</sub>, MgO, TiO<sub>2</sub>, Fe<sub>2</sub>O<sub>3</sub> decrease with increasing silica, while K<sub>2</sub>O and Na<sub>2</sub>O oxides have an ascending trend and Al<sub>2</sub>O<sub>3</sub> remains constant. The increase or decrease in any oxide or element can signify its presence or absence in the minerals constituting the igneous rock. Overall, the variations of the main elements versus SiO<sub>2</sub> in the studied samples indicate a genesis relationship in most of the different intrusive rocks in the Gisel area (Fig. 4).

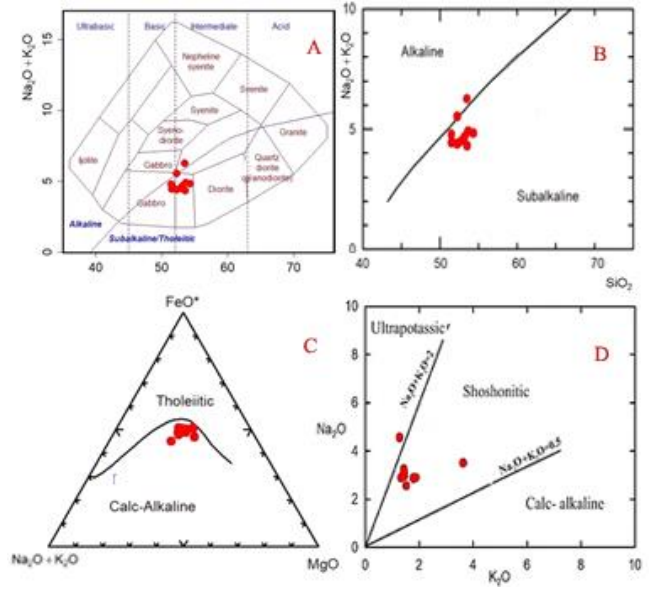


Fig. 4. Plot of gabbroic rocks of the study area on: A and B) Na<sub>2</sub>O + K<sub>2</sub>O versus SiO<sub>2</sub> (Cox et al., 1979 and Middlemost, 1975); C) AFM (Irvine & Baragar, 1971); and D) Na<sub>2</sub>O versus K<sub>2</sub>O (Irvine & Baragar, 1971) diagrams.

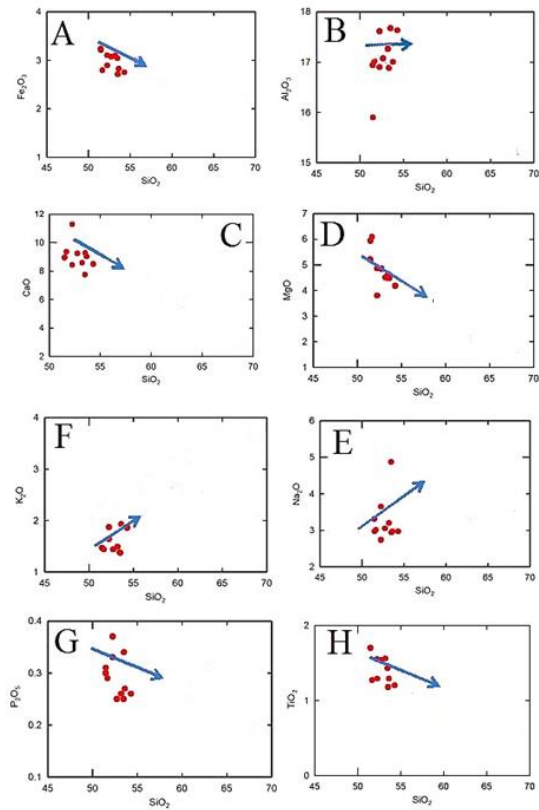


Fig. 5. Variation for major elements in Harker's (1909) diagrams

Using diagrams of variations of rare elements against Th and Zr are of the appropriate methods to understand the magmatic evolution process. The main reason for using Zr in these variations diagrams is because of very low mobility of this

element during alteration and the wide range of variations of this element in basaltic rocks (Le Roex et al., 1983; Meng et al., 2012; Talusani, 2010; Widdowson et al., 2000; Widdowson, 1991). Also, this element shows completely incompatible geochemical behavior during melting and fractional crystallization (FC) in basaltic melts (Talusani, 2010) and has a great affinity to enter and remain in the melt phase. As shown in Fig. 6, the trend of Ni versus Zr is somewhat scattered but negative, while Th versus Hf is somewhat scattered but positive. The trends observed in these diagrams show the consanguinity between the study area rocks and a source origin with almost similar geochemical properties. In addition, the main petrological control is the crystallization process in the basaltic magma of the region. But the cause of the scattering is the abundance of mafic minerals and plagioclases.

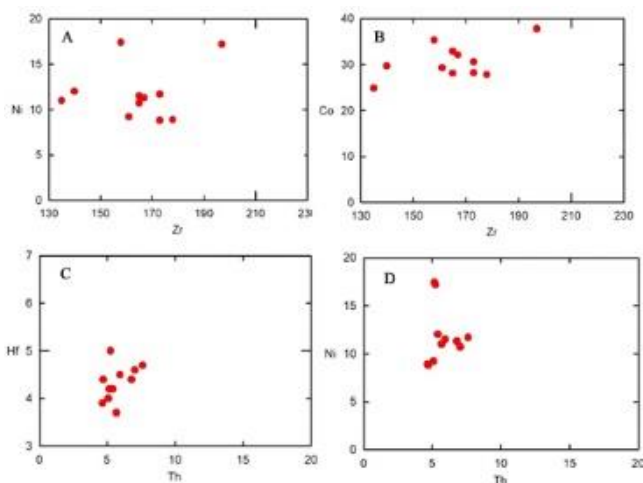


Fig. 6. Variations diagrams of incompatible elements against each other.

Fig. 7 show REE pattern and spider element diagrams of the rocks of the study area. In all diagrams, we can see similar distribution patterns of elements. On the primitive mantle normalized diagrams, some positive and negative anomalies can be seen in the values of Sr, Rb, Nb, Pb, and Ba (Figs. 7A and B). Since Ti and P are high field strength elements (HFSEs) and do not show mobility during secondary processes, their anomalies can be interpreted based on petrological factors. The presence of negative anomalies of Nb also indicates the role of magmatic contamination with the continental crust in the evolution of rocks in the region. Severe positive anomalies of Pb and Ba indicate continental crustal contamination, and a positive Sr anomaly suggests the presence of plagioclase phenocrysts in the rock. The Th positive anomaly is related to the increase of which indicates crustal contamination. On the other hand, the observed depletion of Ti may indicate their subduction zone origin (Gill, 1984).

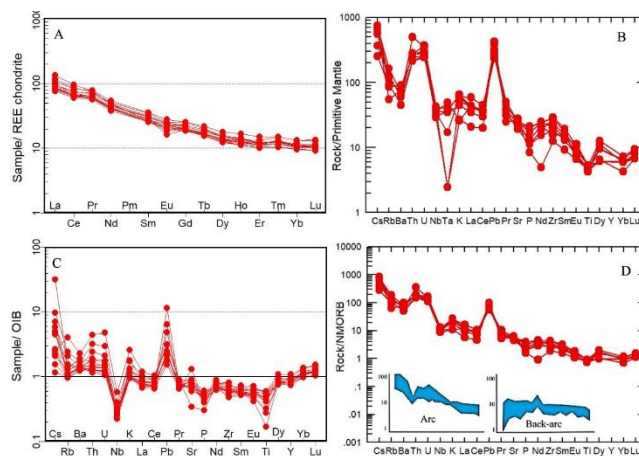


Fig. 7. A) Chondrite-normalized REE pattern (Nakamura, 1974); B) Primary mantle-normalized (Sun and McDonough, 1989); C) OIB-normalized (Sun and McDonough, 1989); D) NMORB-normalized and comparison with the patterns of the magmatic arc and the Japanese evolutionary back-arc (Poulet et al., 1994), diagrams of the studied samples.

High enrichment in Sr, Br, and Rb (Fig. 7) may indicate an association with shoshonitic magma (Morrison, 1980; Jiang et al., 2002). Positive anomalies of Cs compared with primary mantle composition in the studied samples may have resulted from penetration of crustal fluids into the magma or metasomatism of source (MacDonald & Hawakesworth, 2001). The MORB normalized diagrams of these rocks were compared with samples of Japanese magmatic arcs and back-arc basins ones. The similarities and differences between the diagrams indicate the lack of maturity of the back-arc of the study area. According to tectonomagmatic Zr-TH-Nb and Hf-Th-Ta (Wood et al., 1980) diagrams the study area are located in continental arc setting (Fig. 8-A and B), and Cr-Y (Pearce, 1982) diagram the samples are plotted in a volcanic arc setting (Fig. 8-C) but on Zr/Al<sub>2</sub>O<sub>3</sub>-TiO<sub>2</sub>/Al<sub>2</sub>O<sub>3</sub> (Muller et al., 1992) they are laid in continental and post-collision arc zones (Fig. 8-D).

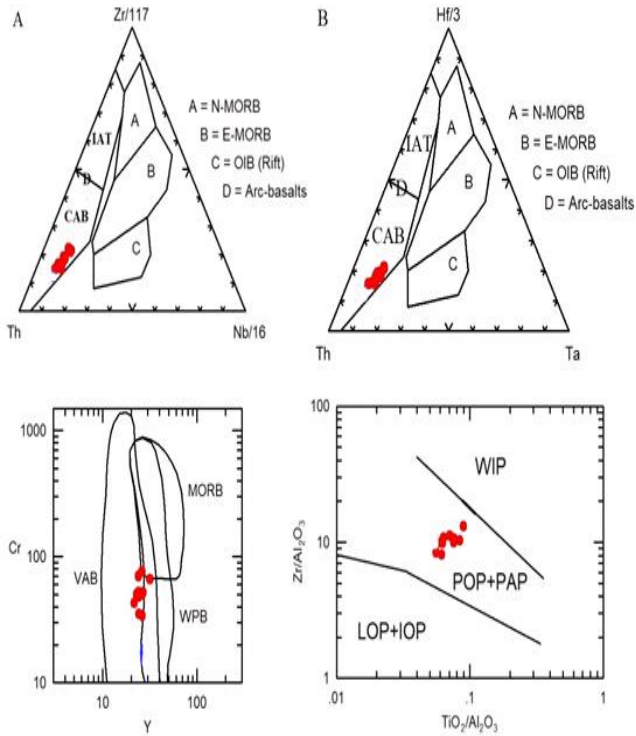


Fig. 8) Plotting of the study area samples on discrimination

diagrams of: A and B) Zr-TH-Nb and Hf-Th-Ta (Wood et al., 1980), C) Cr-Y (Pearce, 1982) and D) Zr/Al<sub>2</sub>O<sub>3</sub>-TiO<sub>2</sub>/Al<sub>2</sub>O<sub>3</sub> (Muller et al., 1992).

On the La/Sm versus La variation diagram (Aldanmaz et al., 2000), the continuous and discontinuous lines show the composition variations trend of the melts with different degrees of melting originating from a spinel-lherzolite and garnet-lherzolite mantle (Fig. 9). The numbers on the lines denote the degree of melting. The range of the depleted and enriched mantle is marked on the thick line. As can be seen, assuming the lherzolite composition of the mantle, the variation trend in the composition of the melt derived from different degrees of mantle melting can be divided into two groups: enriched mantle and depleted mantle. The studied samples, in terms of La and Sm frequencies, all have a similar composition to the melts derived from the enriched mantle and are placed on a process consistent with about 5% melting of garnet-spinel lherzolite. The origin of spinel-lherzolite is also confirmed in the La<sub>N</sub>/Sm<sub>N</sub> diagram versus Tb<sub>N</sub>/Yb<sub>N</sub> (Wang et al., 2008). Based on the location of the rocks studied in this diagram, the mantle composition is often a spinel lherzolite originating from a depth of 60 to 70 km, equivalent to a pressure of 18 to 20 kg, which is in the spinel stability field.

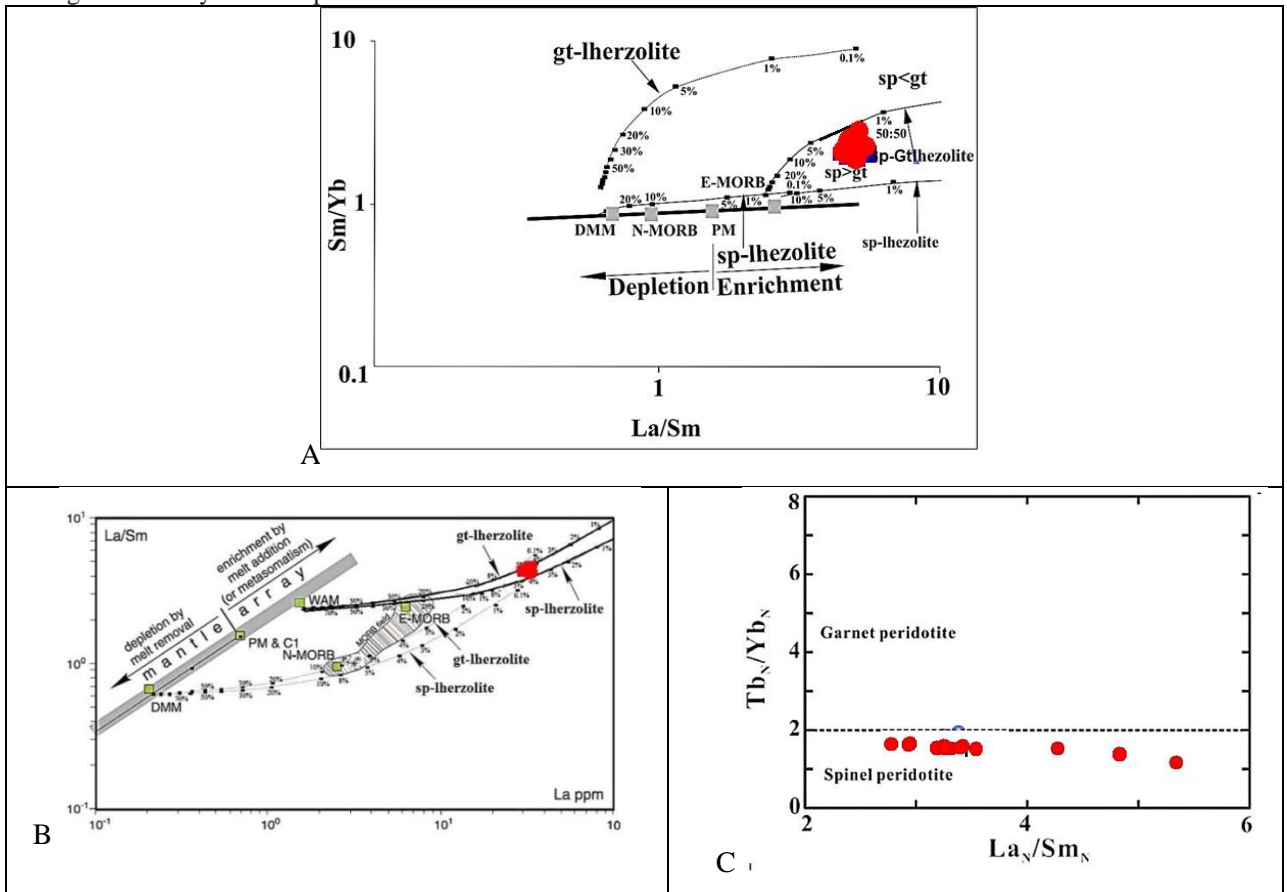


Fig. 9) Study area samples on: A) Sm/Yb versus La/Sm diagram (Shaw, 1970) in which the melting curves are calculated based on the spinel lherzolitic and the garnet lherzolite mantle; B) La/Sm versus La diagram (Aldanmaz et al., 2000); C) Tb<sub>N</sub>/Yb<sub>N</sub> versus La<sub>N</sub>/Sm<sub>N</sub> (Wang et al., 2008) diagram.

Ba is mobile in a wide temperature range, Th is immobile in low-temperature fluids but mobile in high-temperature fluids and mantle melts (Tian et al., 2008; 2011), so Ba/Th to Th/Nb ratios can be used to determine the extent of sediment involvement or the role of fluids in the magma genesis, especially in subduction zones (Tian et al., 2008). On Ba/Th-Th/Nb diagram the high Th/Nb ratio suggests the interference of the released melts due to the partial melting of the sediments at the top of the subducted plate. The high Ba/Th ratio indicates the role of low-temperature aqueous fluids, which may be due to the dehydration of altered oceanic crust or older oceanic sediments. Most of the studied samples have a Th/Nb < 1 so their constituent magma can be considered a result of melting of depleted mantle wedge or lower crust (Fig. 10).

The high content of immobile elements such as Nb and Th in the subduction zone indicates the negligible role of fluids in the magma genesis. Ba has a high solubility in fluids, while the incompatible element Th may be transported by melting resulting from the partial melting of sediments at the top of the subducting plate (Tian et al., 2008; Plank, 2005). The Martynov et al. (2007) diagram shows that the melt resulting from the partial melting of the sediments above the subducted plate plays a greater role than the fluids (Fig. 10).

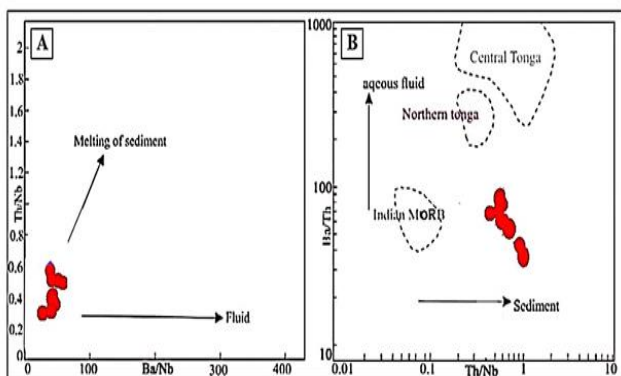


Fig. 10. Studied samples on the role of subduction constituents diagrams (fluid/melt): A) Th/Nb versus Ba/Th (Tian et al., 2008); B) Ba/Nb versus Th/Nb (Martynov et al., 2007)

The Ce/Yb ratio can indicate the depth and melting rate of the parental rock. A small value of this ratio (< 15) indicates that the magma has originated from the upper parts of the mantle (low depth or high melting rate). In contrast, magmas with a Ce/Yb > 15 indicate that the magma has originated from depths with low melting rate (high pressure) (Cotton et al., 1995). Ce/Yb in the intrusive masses of the region is about 25.71, indicating the samples' high depth and low melting degree. Also, according to Conly et al. (2005), Rb/Zr > 0.12 indicates a mantle source affected by metasomatism. Overall, this ratio is about 0.26 in the rocks of the study area.

In the studied intrusive rocks, Nb/Ba and Th/Nb increase with increasing Yb/Ba and Th/Yb, respectively. The positive

correlation between these ratios indicates the similarity of the studied samples with the newly enriched back arc basalts and their difference with the new island arc basalts, which have a negative correlation between Ba/Nb and Ba/Yb (Li et al., 2013) (Fig. 11). In this study, the source enrichment degree of the studied rocks was determined using the ratios of incompatible elements Zr/Y and Zr/Nb (McDonough & Sun, 1989). Since Zr and Nb behave are incompatible during the fractional crystallization of olivine, pyroxene, magnetite, and plagioclase in basaltic magmas, they are suitable representatives for the composition of the source site (Reichow et al., 2005). Based on these ratios, the source of all studied samples is the enriched mantle (Fig. 11). Here, Sm is incompatible with Yb in the mantle. Also, because it exists in the pyroxene structure and, if present, in the amphibole structure, its concentration compared to Yb varies sharply during the melting processes in the mantle (Li & Che, 2014). Hence, Sm/Yb can be used to determine the mantle chemical composition (Aldanmaz et al., 2000). In the Sm/Yb versus Ce/Sm diagram, which is designed to detect the presence or absence of garnet at the source of melt generation, the samples are in the garnet range and prove the presence of garnet at the source of these rocks (Fig. 11).

Geochemistry of REEs is widely used to determine the degree of partial melting and the depth of primary mantle magmas (Rollinson, 1993; Zhou, 2007; Furman & Zhao, 2007). The Sm/Yb versus Sm diagram (Li & Chen, 2014) shows changes in the degree of partial melting at two mantle origins of peridotite spinel and peridotite garnet. In this diagram, the Sm/Yb and Sm ratios decrease with increasing the degree of partial melting. The basalt rocks studied in this diagram fall in the peridotite garnet melting curve with a partial melting point of 1 to 10% (Fig. 11F). In the studied samples, the depth obtained for the melting site of the mother magma using the Ce versus Ce/Yb diagram is 100 to 110 km (Ellam, 1992).

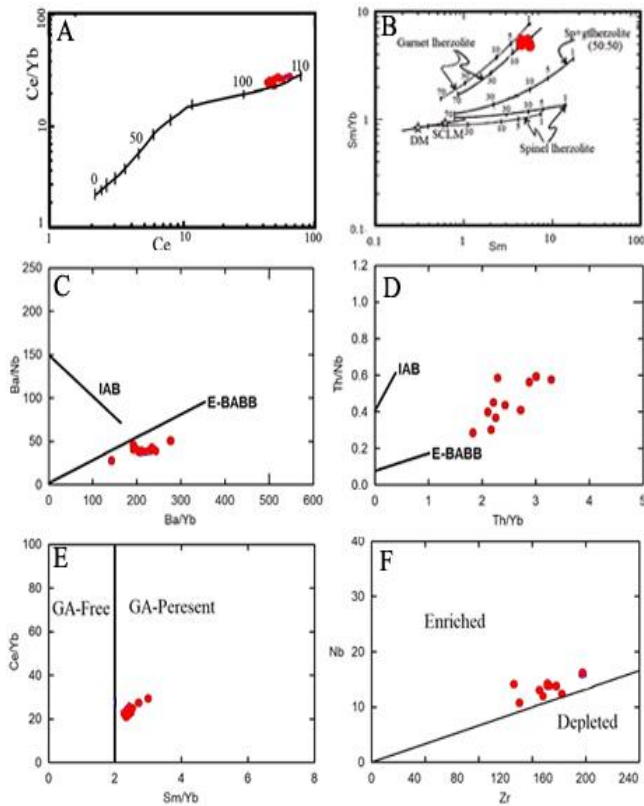


Fig. 11. Study area samples on: A) Li & Chen (2014); B) Ellam (1992); C and D) Li et al. (2013) E) Sun & McDonough (1989); F) Coban (2007) diagrams.

Presenting a geodynamic model for the genesis of igneous rocks in the study area

Based on the shoshonite nature of the studied samples and information on Fig. 12-A, the tectonic setting of these rocks is post-collision arcs. Subduction-related magmas generally show depletion from Ti, Nb, and Ta (Baier et al., 2008). However, arc zones show common features with subduction zones as they are depleted of HILEs (i.e., Ti, Ta, and Nb) and enriched in LILEs and Sr (Pearce et al., 1984). Fig. 12-B presents the data of the study area in the Nb/Yb diagram versus Th/Nb. The chart also illustrates data from Pouclet et al. (1994) to distinguish between back-arc basin basalts (BABBs), oceanic island basalts (OIB), and arc basalts of the Sea of Japan. This diagram shows that all samples in the arc-dependent part of the Japanese pattern.

We used the Yb versus La/Yb diagram to investigate the type of arcs in the Gisel region (Fig. 12-C). This diagram shows that the studied rocks do not fit in the normal or adakitic arc range. This group of Eocene post-collision arcs has been reported from Alborz to parts of the southern Caucasus and southern Armenia (Moritz et al., 2015). There is ample evidence about the pre-Eocene Alborz to southern Armenia extension of the post-Eocene transpressive phase, the Lesser Caucasus and Alborz to extensive deformation in the form of folds and shortening, and cessation of magmatism in many studies (Vincent et al., 2005; Sosson et al., 2010; Brunet et al., 2003). According to the data and

studies, the rocks of the Gisel region have been formed in an extensional post-collision basin.

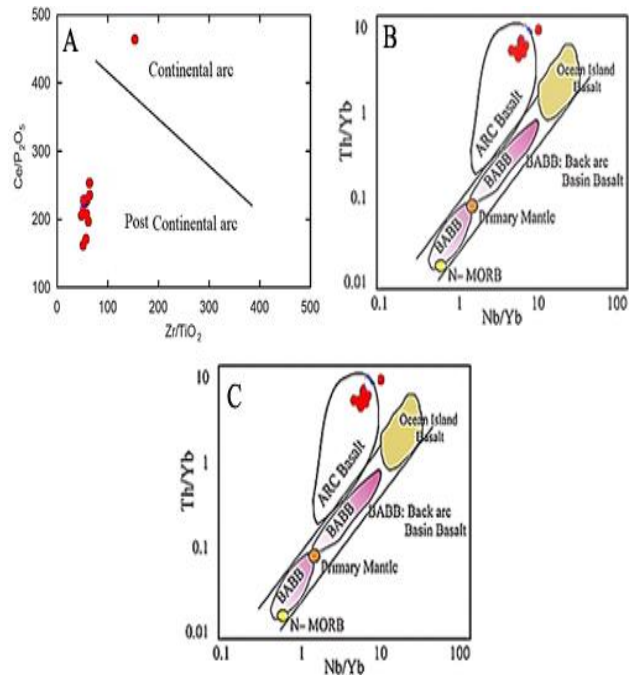


Fig. 13. Studied samples on: A) Muller & Groves (1997); B) Pouclet et al. (1994); C) Defant and Drummond (1990) diagrams.

## Conclusion

This study showed that rock units of the region include intrusive masses and have an subalkaline nature. Based on lithographic studies, their texture is granular, intergranular, poikilitic, and porphyritic. Geochemical studies indicate the formation of the magma of these rocks from the partial melting of 2 to 5% of a mantle source of peridotite garnet during the uplifting at a depth of 100 to 105 km. The results also show the important role of fractional crystallization as the main process in the formation of the parental magma of these rocks. According to tectonic diagrams and tectonomagmatic studies, the Gisel area rocks have been formed in a post-collision extensional basin.

## REFERENCES

1. Agard P., Omrani J., Jolivet L., Whitechurch.H., Vrielynck B., Spakman W., Monie P., Meyer
2. Aldanmaz, E., Pearce, J. A., Thirlwall, M. F. & Mitchell, J. G., 2000- Petrogenetic evolution of late Cenozoic, post-collision volcanism in western Anatolia, Turkey. *Journal of Volcanology geothermal Research* 102: 67-95.
3. Allen, M. B., Ghassemi, M. R., Shahrabi, M. & Qorashi, M., 2003- Accommodation of Late Cenozoic oblique shortening in the Alborz range, northern Iran", *Journal of Structural Geology* 25: 659-675.
4. Annells, R.N., Arthurton, R.S., Bazely, R.A. and Davies, R.G. 1975. Explanatory text of the Qazvin and Rasht quadrangle map1:250000, G.S.I. Rep., nos. E3, E4, 94p.
5. Asiabanha A., 2001 "Geology and petrogenesis of volcanic facies at the Uzbashichai area, west of Qazvin", PhD thesis, University of

- Tarbiyat Modares, p: 321.
6. Asiabanha A., Ghassemi H., Meshkin M., 1989 "Paleogene continental-arc type volcanism in
  7. Asiabanha, A., Foden, F., 2012. Post-collisional transition from an extensional volcano-sedimentary basin to a continental arc in the Alborz ranges, N-Iran, *Lithos*, 148, 98–111.
  8. B., Wortel R., 2011. "Zagros orogeny: a subduction-dominated process", *Geological Magazine*, Vol: 148, (2011) p: 692-725.
  9. Baratian, M.; Arian, M.A.; Yazdi, A. (2018) Petrology and petrogenesis of the SiahKuh intrusive Massive in the South of KhoshYeilagh, *Amazonia Investiga*, 7 (17), 616-629
  10. Berberian, F. & Berberian, M., 1981- Tectono-plutonic episodes in Iran. In: Gupta HK, Delany FM (eds) *Zagros, Hindukosh, Himalaya Geodynamic Evolution*. American Geophysical Union, Washington DC: 5–32.
  11. Bina, M.; Arian, M.A.; Pourkermani, M.; Bazoobandi, M.H.; Yazdi, A. (2020). Study of the petrography and tectonic settings of sills in Lavasanat district, Tehran (north of Iran), *Nexo Revista Cientifica*, v.33(2), p. 286-296. DOI: <https://doi.org/10.5377/nexo.v33i02.10768>
  12. Conly, A. G., Bernan, J. M., Bellon, H. and Scott, S. D., 2005- Arc to rift transitional volcanism in the Sanata Rosalia Region, Baja California Sur, Mexico. *Journal of Geology* 72: 303-341.
  13. Cotton, J., Le, Dez A., Bau, M., Caroff, M., Maury, R. C., Dulski, P., Fourcade, S., Bohn, M. and Brousse, R. 1995- Origin of anomalous rare earth element and yttrium enrichments in subaerially exposed basalts, evidence from French Polynesia. *Chemical Geology* 119: 115-138.
  14. Cox, K. G., Bell, J. D., Pankhursts, R. J., 1979, The interpretation of igneous rocks. George Allen and Unwin., PP 450.
  15. Defant, M. J. and Drummond, M. S., 1990- Derivation of some modern arc magmas by melting of young subducted lithosphere. *Nature* 347:662–665.
  16. Ershov, A. V., Brunet, M. F., Nikishin, A. M., Bolotov, A. N., Nazarevich, B. P. & Korotaev, M. V., 2003- "Northern Caucasus Basin: thermal history and synthesis of subsidence models", *Journal of Sedimentary Geology* 156: 95-118.
  17. Furman, T., 2007- Geochemistry of East African Rift basalts: An overview. *Journal of African Earth Sciences* 48: 147-160.
  18. Gharib-Gorgani, F.; Ashja-Ardalan, A.; Espahbod, M.R.; Sheikhzakariaee, S.J.; Yazdi, A. (2017). Petrology of Mg-bearing Meta Ophiolite Complexes of Qaen-Gazik, Eastern Iran, *National Cave Research and Protection Organization*, v. 4(1), DOI:10.21276/ambi.2017.04.1.ga01
  19. Ghasemi, A. & Talbot, C. J., 2006- A new tectonic scenario for the Sanandaj–Sirjan Zone (Iran). *Journal of Asian Earth Sciences* 26: 683–693.
  20. Glazner, A. F., and W. Ussler III (1989), Crustal extension, crustal density, and the evolution of Cenozoic magmatism in the Basin and Range of the western United States, *J. Geophys. Res.*, 94, 7952–7960, doi:10.1029/JB094iB06p07952.
  21. Guest, B., Axen, G.J., Lam, P.S., Hassanzadeh, J., 2006a. Late Cenozoic shortening in the west–central Alborz Mountains, northern Iran, by combined conjugate strike–slip and thin–skinned deformation. *Geosphere*, 2: 35–52.
  22. Guest, B., D. F. Stockli, M. Grove, G. J. Axen, P. S. Lam, and J. Hassanzadeh (2006b), Thermal histories from the central Alborz mountains, northern Iran: Implications for the spatial and temporal distribution of deformation in northern Iran, *Geol.Soc. Am. Bull.*, 118, 1507–1521, doi:10.1130/B25819.1.
  23. Heuret, A., and S. Lallemand (2005), Plate motions, slab dynamics and back-arc deformation, *Phys. Earth Planet. Inter.*, 149, 31–51.
  24. Heuret, A., Lallemand, S., 2005, Plate motions, slab dynamics and back-arc deformation, *Journal of Physics of the Earth and Planetary Interiors* 149. 31–51.
  25. Humphreys, E., E. Hessler, K. Dueker, G. L. Farmer, E. Erslev, and T. Atwater (2003), How Laramide-age hydration of North American lithosphere by the Farallon slab controlled subsequent activity in the western United States, *Int. Geol. Rev.*, 45, 575–595, doi:10.2747/0020-6814.45.7.575.
  26. Irvin, T., Baragar, W.R.A., 1971, A guide to the Chemical classification of the common volcanic rocks. *Canadian Journal of earth Science Letters.*, Vol. 8, PP: 523-548.
  27. Jehangir Khan, M.; Ghazi, S.; Mehmood, M.; Yazdi, A.; Naseem, A.A.; Sarwar, U.; Zaheer, A.; Ullah, H. (2021). Sedimentological and provenance analysis of the Cretaceous Moro formation Rakhi Gorge, Eastern Sulaiman Range, Pakistan, *Iranian Journal of Earth Sciences*, v.13 (4), p. 251-265. doi: 10.30495/ijes.2021.1917721.1564
  28. Kelemen, P.B., Kikawa, E., Miller, D.J., and Shipboard Science Party, 2004, *Proceedings of the Ocean Drilling Program, Initial reports, Volume 29: College Station, Texas, Ocean Drilling Program*, doi: 10.2973/odp.proc.ir.209.
  29. Le Roex, A. P. Dick H. J. B. Erlank A. J. Reid A. M. Frey F. A. and Hart S. R., 1983, Geochemistry, mineralogy and petrogenesis of lavas erupted along the south west Indian ridge between the Bouvet triple junction and 11 degrees east. *Journal of Petrol.*, Vol. 24, PP. 267-318.
  30. Li, B., Bagas, L., Gallardo, L. A., Said, N., Diwu, C. & McCuaig, T. C., 2013- Back-arc and post-collisional volcanism in the Palaeoproterozoic Granites-Tanami Orogen, Australia. *Precambrian Research* 224: 570– 587.
  31. Li, Z. & Chen, B., 2014- Geochronology and geochemistry of the Paleoproterozoic meta-basalts from the Jiao-Liao-Ji Belt, North China Craton: Implications for petrogenesis and tectonic setting. *Precambrian Research* 255: 653–667.
  32. Martynov, Y.A., Kimura, J.I., Khanchuk, A.I., Rybin, A.V., Chashchin, A.A., 2007. Magmatic sources of Quaternary lavas in the Kuril island arc: New data on Sr and Nd isotopy. *Doklady Earth Sciences*, 417, 8, 1206-1211.
  33. Middlemost, E. A. K., 1985. *Magma and magmatic rocks*, An Introduction to igneous petrology. Longman Group U.K., PP 73 – 86.
  34. Mobashergarmi M., 2013 "Petrological, petrographical and geochemical studies of basaltic rocks in south Germei (Ardabil province)", MSc thesis, University of Tabriz, Tabriz, Iran, (in Persian).
  35. Muller, D. & Groves, D.I., 1997. "Potassic igneous rocks and associated gold-copper mineralization", Sec. Updated, Springer Verlag, p. 242.
  36. Nakamura, N., 1974, Determination of REE, Ba, Fe, Mg, Na and K in carbonaceous and ordinary chondrites. *Geochim Cosmochim Acta.*, Vol. 38, PP. 757-775.
  37. Nemati B., Asiabanha A., 2017 "Volcano-plutonic relations in Lat-Bolukan district (North of Qazvin, Western Alborz): Petrogenetic analysis and geochemical modeling", *Journal of Petrology*, Vol: 8 (31), p: 167-180.
  38. north Qazvin, north Iran: facies analysis and basalts as petrogenetic indicator". *Chemical Geology*, Vol: 77(3), p: 165-182.
  39. Pearce, J. A., 1982 "Trace element characteristics of lavas from destructive plate boundaries" John Wiley and Sons, U.K., pp. 525–548. 177–195. 28: 2023-2037.
  40. Plank, T., and C. H. Langmuir (1988), An evaluation of the global variations in the major element chemistry of arc basalts, *Earth Planet. Sci. Lett.*, 90, 349–370, doi: 10.1016/0012-821X(88)90135-5.
  41. Rahimi G., Kananian A., Asiabanha A. 2010. "Tectonic setting and petrogenesis of post-Eocene
  42. Rollinson, H. R., 1993- *Using Geochemical Data: Evaluation, Presentation, Interpretation*. John Wiley and Sons, 325p.
  43. Shafaii Moghadam M.H., Shahbazi Shiran S.H., 2010. "Geochemistry and petrogenesis of volcanic rocks from the northern part of the Lahrud region (Ardabil): an example of shoshonitic occurrence in northwestern Iran". *Journal of Petrology*, Vol: 1(4).16-31 (in Persian).
  44. Shaw, D.M., 1970, Trace element fractionation during anatexis, *Geochim. Cosmochim. Acta*, 34, 237-243.
  45. Stampfli, G., 1978. *Etude geologique generale de l'Elburz oriental au S de Gonbad-e-Qabus (Iran, N-E): These de Docteur des Sciences*, no. 1868. Universite de Geneve. pp.328.
  46. Stöcklin J., 1974 "Northern Iran: Alborz Mountains. In: *Mesozoic–Cenozoic orogenic belts: data for orogenic studies*", (Ed. Spencer, A.) Vol: 4, p: 213–234.
  47. Sun, S. S. and McDonough, W. F., 1989, Chemical and isotopic systematics of oceanic basalts: implications for mantle composition and processes" In: Saunders, A.D., Norry, M.J. (Eds.), *Magmatism in the Ocean Basins*. *Geol Soc Spec Publ.*, Vol. 42, PP. 313-345.
  48. Sun, S. S. and McDonough, W. F., 1989, Chemical and isotopic

- systematics of oceanic basalts: implications for mantle composition and processes" In: Saunders, A.D., Norry, M.J. (Eds.), *Magmatism in the Ocean Basins*. Geol Soc Spec Publ., Vol. 42, PP. 313-345.
49. Talusani V. R., 2010, Bimodal tholeiitic and mildly alkalic basalts from Bhir area, central Deccan Volcanic Province, India: Geochemistry and petrogenesis. *Journal of Volcanol. Geotherm. Res.*, Vol. 189, PP. 278-290.
  50. Teimouri S., Ghasemi H., Asiabanha A., 2018. "The role of crustal contamination and differentiation in the formation of the Eocene volcanic rocks in Jirande area (Northwest of Qazvin)", *Journal of Petrology*, Vol: 9 (33), (2018) p: 71-90.
  51. Tian, H. Q., et al. 2008, Forecasting and assessing the large-scale and long-term impacts of global environmental change on terrestrial ecosystems in the United States and China, in *Real World Ecology: Large-Scale and Long-Term Case Studies and Methods*, edited by S. Miao, S. Carstenn, and M. Nungesser, pp. 235– 266, Springer, New York.
  52. Tian, H., Melillo, J., Lu, Ch., Kicklighter, D., Liu, M., Ren, W., Xu, X., Chen, G., Zhang, C., Pan, S., Liu, J., Running, S., 2011. China's terrestrial carbon balance: Contributions from multiple global change factors. *Global Biogeochemical Cycles*. V 25.
  53. Valizadeh M.V., Abdollahi H.R., Sadeghian M., 2008. "Geological investigations of main intrusions of the Central Iran", *Geosciences Scientific Quarterly Journal*, Vol: 17(67), (2008) p: 182-197 (in Persian).
  54. Verdel, C., Wernicke, B.P., Hassanzadeh, J., 2011, A Paleogene extensional arc flare-up in Iran, *Tectonics*, 30, Issue 3.
  55. volcanic rocks of Abazar district (NE of Qazvin)", *Journal of Crystallography and Mineralogy*, Vol:18(2), (2010) p: 167-180 (in Persian).
  56. Wang, YN., Zhang, C. J., Xiu, SZ., 2001, Th/Hf-Ta/Hf identification of tectonic setting of basalts. *Acta Petrol Sin(in Chinese).*, Vol. 17(3), PP. 413-421.
  57. Widdowson, HG., 1991, *Aspects of Language Teaching*. Oxford: OUP (1996). *Teaching Language as Communication*. Oxford: OUP. p 160.
  58. Widdowson, M., Pringle M. S. and Fernandez O. A., 2000, A post K-T Boundary (Early Palaeocene) age for Deccan-type feeder dykes, Goa, India" *J Petrol.*, Vol. 41, PP. 1177-1194.
  59. Wood, D. A., 1980, The application of a Th-Hf-Ta diagram to problems of tectonomagmatic classification and to establishing the nature of crustal contamination of basaltic lavas of the British Tertiary volcanic province. *Earth Planet Sc Lett.*, Vol. 50, PP. 11-30.
  60. Yazdi A.; Shahhosseini, E.; Moharami, F. (2022) Petrology and tectono-magmatic environment of the volcanic rocks of West Torud–Iran, *Iranian Journal of Earth Sciences* 14 (1): 40-57
  61. Yazdi, A.; Ashja-Ardalan, A.; Emami, M.H.; Dabiri, R.; Foudazi, M. (2019-a). Magmatic interactions as recorded in plagioclase phenocrysts of quaternary volcanics in SE Bam (SE Iran), *Iranian Journal of Earth Sciences*, v.11(3), p. 215-224. DOI: [http://ijes.mshdiau.ac.ir/article\\_667379.html](http://ijes.mshdiau.ac.ir/article_667379.html)
  62. Yazdi, A.; ShahHoseini, E.; Razavi, R. (2016). AMS, A method for determining magma flow in Dykes (Case study: Andesite Dyke). *Research Journal of Applied Sciences*, v. 11(3), p. 62-67
  63. Yazdi, A.; Ashja Ardalan, A.; Emami, M.H.; Dabiri, R.; Foudazi, M. (2019-b). Magmatic interactions as recorded in plagioclase phenocrysts of quaternary volcanics in SE Bam (SE Iran), *Iranian Journal of Earth Sciences* v.11 (3), p.215-225.
  64. Yazdi, A.; sharifi teshnizi, E.; Effects of contamination with gasoline on engineering properties of fine-grained silty soils with an emphasis on the duration of exposure, Springer, *SN Applied Sciences* 3. (2021). 704. DOI: <https://doi.org/10.1007/s42452-021-04637-x>
  65. Zanchi, A., Berra, F., Mattei, M., Ghassemi, M. R. & Sabouri, J., 2006- "Inversion tectonics in Central Iran", *Journal of Structural Geology* 28: 2023-2037.
  66. Zanchi, A., Berra, F., Mattei, M., Zanchetta, S., Nawab, A. and Sabouri, J. (2005) The early Mesozoic Cimmerian orogeny in the Alborz mountains, Iran. *Geophysical Research* 7: 1607-7962.
  67. Zhao, J. H. & Zhou, M. F., 2007. Geochemistry of Neoproterozoic mafic intrusions in the PanzihuaNdistrict (Sichuan Province, SW China): Implications for subduction-related metasomatism in the upper mantle. *Journal of Precambrian Research* 152: 27-47.